Photonic crystal multiple diffraction observed by angular-resolved reflection measurements

Alexander Tikhonov, Justin Bohn, and Sanford A. Asher*
Department of Chemistry, University of Pittsburgh, Pittsburgh, Pennsylvania 15260, USA
(Received 2 June 2008; published 17 December 2009)

Angular-resolved reflection measurements suggest that higher-order Miller-index crystal planes of a fcc photonic crystal reflect specularly about the normal to the (111) planes. We suggest that this phenomenon results from a two-step diffraction process where light is first Bragg diffracted by higher-order Miller-index crystal planes and is then two-dimensionally diffracted by periodicities within the (111) planes to produce the specularly diffracted light. This phenomenon is a three-dimensional analog of the well-known Wood's anomaly.

DOI: 10.1103/PhysRevB.80.235125 PACS number(s): 42.25.Fx, 42.72.−g, 78.67.−n, 92.60.Ta

Photonic crystal materials (PhC) are being developed for use in optical devices and for applications in optical computing and optical communications, with the expectation that photonic circuitry will replace electronic circuitry.[1] The periodic modulations of the optical dielectric constant in these PhC materials are used to control the propagation of electromagnetic radiation at wavelengths comparable to the modulation periodicity.[2,3]

Obviously, it is essential to develop a deep understanding of the interaction of light with these PhC materials. Although there have been numerous studies which have examined diffraction from PhC, significant aspects of the diffraction phenomena remain unclear.

Many previous studies examined diffraction from PhC using angularly resolved reflection or transmission spectroscopy.[4–17] These studies observed complex patterns of peaks or dips in diffraction intensities which depend upon the angle of incidence and observation. The diffraction phenomena give rise to diffraction dispersion spectra. Two approaches are used to rationalize the origin of these diffraction dispersion spectra. The first relates these experimental diffraction dispersion spectra to the allowed photonic bands determined from band-structure calculations.[4–7,9–12,17] The second relates these diffraction dispersion spectra to the Bragg diffraction phenomena expected from particular crystal planes.[4,6–8,12–15]

Good correlations have been obtained between some experimental diffraction dispersion spectra and low-energy photonic bands associated with diffraction from the (111) and (200) planes.[5–7,11–14] These lower-energy photonic bands follow the wavelength versus angular dependence predicted by Bragg's law in regions away from band crossings. However, in the region where the (111) and (200) photonic bands cross, multiple Bragg wave-coupling results in the repulsion of these two bands and deviations from Bragg's law.[5] The situation is more complex at higher frequencies, where higher-frequency dispersion lines poorly correlate to the photonic bands found from band-structure calculations.[10,11]

A number of groups examined higher-energy dispersion spectra in relatively low-contrast PhC and found that, in general, the dispersions can be fit to Bragg's law. Watson and co-workers were able to fit five diffraction dispersion lines in a bcc PhC measured with transmission spectroscopy to diffraction from higher-order Miller-index planes.[8] Schutzmann *et al.*[6] were able to fit four reflection diffraction dispersion lines for fcc PhC. However, they did not discuss why their higher-order Bragg diffraction should occur at angles which are specular to the fcc (111) planes. Numerous groups have been trying to understand why the diffraction from higher-order Miller-index planes should appear specular to the (111) planes.[4–16] The explanation by Miguez *et al.*[10] proposes that flattening of the photonic bands as a function of wave vector **k** results in a large effective refractive index, n_{eff}, which leads to a high reflectivity at the sample surface at the Bragg diffraction condition. This argument does not clarify why this diffraction would have the wavelength versus angle dependence given by Bragg's law.

In a work by Baryshev *et al.*[14] the authors propose a multiple diffraction mechanism to explain how incident light diffracted by the (−111) planes is redirected to give an intensity peak in the specularly reflected direction. In their mechanism the incident light is diffracted by (−111) planes of the twinned fcc structure in the direction parallel to the surface and then diffracted again by the (−111) planes of the twin into the specular reflection direction. Their mechanism can apply only to light incident at 46° in the L-K-U scanning plane. In contrast, we observe intensity peaks corresponding to diffraction by the (020), (220), (11-1), (13-1), (202), (113), and (224) planes in the range of incident angles between 20° and 70°. Other groups have also observed these diffraction dispersion lines over a broad range of incident angles. The mechanism suggested by Baryshev *et al.* clearly does not explain dispersion lines observed over this broad range of incident angles.

We further examine these phenomena here by studying the angular-resolved reflection spectra from highly ordered fcc crystalline colloidal array (CCA) PhC oriented with their (111) planes parallel to the PhC flat surface. Our low dielectric constant modulated PhC displays eight diffraction dispersion lines; as far as we know, this is the largest number yet observed. We introduce a simple phenomenological model to explain the origin of the reflection spectroscopy peaks in the high-frequency region as a multiple diffraction phenomenon.

We propose that each dispersion line occurs as a result of two consecutive scattering processes: in the first scattering process, the incident light is three-dimensional (3D) Bragg diffracted by a set of crystal planes. In the second scattering process this Bragg diffracted wave is two-dimensional (2D) diffracted by the 2D periodicity within the surface (111) planes. The resulting diffracted light propagates as if it was

specularly reflected relative to the incident light. We suggest that this phenomenon is similar to that known for one-dimensional (1D) systems as a Wood's anomaly.[18–22]

In our study we examine two nonclose-packed fcc CCA samples made from 198 nm highly charged spherical polystyrene colloidal particles suspended in water. The particles were prepared as described elsewhere.[23] CCA self-assemble due to the electrostatic repulsion between the charged particles[24] into either an fcc or bcc crystal depending on particle number density and surface charge.[25] The fcc CCA samples were injected into a 700-μm-thick borosilicate glass flow cell. These CCA align their highest density (111) planes parallel to the cell surface. We measured the reflection spectra of the CCA sample for unpolarized light over the angular range of $20°-70°$ about the normal to the fcc (111) planes in the LU (LK) (Ref. 26) and LW Brillouin-zone rotation directions. Variable-angle specular-reflectance data were measured by using a Cary 5000i spectrophotometer equipped with a variable-angle specular-reflectance accessory (Varian Inc.). The angular resolution was set at 2°, the beam area at the CCA sample was 1 cm^2, and the collection angular aperture was 8°.

At normal incidence to the (111) planes the high particle concentration CCA sample shows the longest-wavelength Bragg diffraction at 682 nm while the low-concentration CCA sample diffracts 1078 nm light. We calculated the CCA lattice constant and effective average refractive index from a linear best fit of the (111) Bragg diffraction wavelengths for different angles of incidence to the experimental lowest-energy dispersion line. Fitting of the (111) Bragg diffraction including light refraction was done assuming constant values of the refractive index of water and polystyrene. The lattice constants and effective average refractive indices were 429 nm and 1.380 for the high-concentration CCA, and 695 nm and 1.343 for the low-concentration CCA. We took cognizance of the wavelength dependence of the refractive index of water and polystyrene when fitting the higher-order Miller-index dispersion lines. We used the same fitted effective refractive index for both the Bragg's law calculation and for the Snell's law correction for refraction of incident light at the CCA surface.

Figure 1 shows the diffraction dispersion lines obtained over the LW Brillouin-zone directions for the high- and low-concentration CCA samples. The most intense diffraction dispersion line from the (111) planes follows Bragg's law up to the (111) and (200) dispersion line crossing point.

The other dispersion lines follow Bragg's law calculated fits (white lines) as if the incident light diffracted from one of the higher-order Miller-index planes where the diffracted light was somehow directed in the specular reflection direction. The dispersion line fits to the higher Miller-index planes cannot simply derive from a simple 3D Bragg diffraction since the incident light would not be diffracted in the specular reflected direction.

The expected diffraction from PhC should result in bright spots at specific angular directions which overlay a diffuse background scattering from defects and disorder. These bright diffraction spots result from 3D Bragg diffraction from crystal planes and from 2D diffraction from the surface layers.[27,28]

In reflection we often observe a hexagonal pattern of six 2D diffraction spots from the (111) layers near the surface. The total light intensity in each 2D diffraction spot results from partial constructive interference of diffraction by all of the (111) layers.[27] For a simple Bravais lattice, 3D Bragg diffraction can be considered as a special case of 2D diffraction where the scattered light amplitudes from every layer are in phase and constructively interfere.

As shown quantitatively below, the appearance of the higher-frequency specular-reflection dispersion lines in Fig. 1 involves a multiple diffraction phenomenon. Two consecutive diffraction events are required for an incident monochromatic beam to diffract from a higher-order Miller-index planes and to exit the PhC in the specularly reflected direction about the (111) plane normal (Fig. 2). When the PhC is illuminated at the Bragg diffraction condition for a specific crystal plane, some of the incident light is redirected into a Bragg diffracted wave propagating inside the PhC. Then this wave 2D diffracts off (111) layers into several diffraction orders, one of which is diffracted into the specular reflected direction.

Figure 2(a) shows the calculated 2D and 3D (200) Bragg diffracted beams for an incident monochromatic beam at an *internal* angle 10° to the (111) plane normal that is Bragg diffracted by the (200) planes. The incident-beam wave vector $\vec{k}_{in}$ and the 3D Bragg diffracted beam wave vector $\vec{k}_{sc}$ define the scattering plane containing the (200) plane normal (red arrows). In addition to this 3D Bragg diffraction, weaker 2D diffraction occurs from the surface (111) planes, generating a number of 2D diffracting beams (four beams for our specific scattering geometry) with wave vectors $\vec{k}^{2D}_{sc}$ (blue arrows). We use the (200) set of planes as an example here but the analyses is valid for all crystal planes.

Figure 2 shows two first-order 2D diffraction beams, one of which coincides with the (200) 3D diffraction direction. There are also two additional zero-order 2D diffracted beams which propagate in the transmitted and (111) specularly reflected directions.

We will prove that if the 3D Bragg condition occurs, the 2D diffraction condition will also occur, by proving that the projection of the 3D reciprocal lattice vector of the (200) planes, $\vec{G}_{200}$ onto the (111) plane coincides with a 2D reciprocal lattice vector within the (111) plane. We will then show that the 3D diffracted beam can be further diffracted by a 2D reciprocal lattice vector resulting in a 2D diffracted beam which propagates as if it were specularly reflected from the (111) planes.

The 2D periodicity within a particular crystal plane is defined by two primitive 2D lattice vectors $\vec{a}$ and $\vec{b}$ while the 3D periodicity of the fcc lattice is defined by its 3D primitive lattice vectors $\vec{A}$, $\vec{B}$, and $\vec{C}$. The set of 2D reciprocal lattice vectors, $\vec{G}^{2D}$, within a particular lattice plane satisfies the two Laue equations $\vec{a}\cdot\vec{G}^{2D}=2\pi m_1$ and $\vec{b}\cdot\vec{G}^{2D}=2\pi m_2$ while the 3D reciprocal lattice vectors of the 3D lattice satisfies the three Laue equations $\vec{A}\cdot\vec{G}=2\pi n_1$, $\vec{B}\cdot\vec{G}=2\pi n_2$, and $\vec{C}\cdot\vec{G}=2\pi n_3$. Since the individual crystal planes are part of the 3D lattice we can write $\vec{a}=a_1\vec{A}+a_2\vec{B}+a_3\vec{C}$ and $\vec{b}=b_1\vec{A}+b_2\vec{B}+b_3\vec{C}$, where (a_1,a_2,a_3) and (b_1,b_2,b_3) are integers. There-

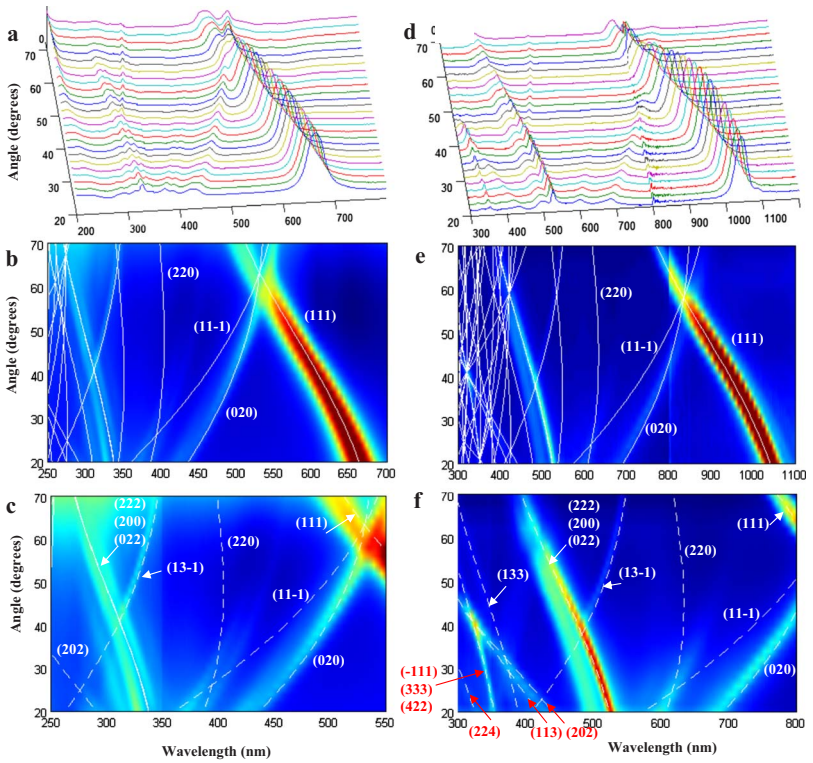

FIG. 1. (Color online) Reflection spectra along the LW Brillouin-zone direction for [(a)–(c)] high-concentration and [(d)–(f)] low-concentration CCA. The calculated Bragg dispersions lines are plotted on the experimental data contour plots. (c) and (f) show expanded versions of (b) and (e) and show only the calculated Bragg dispersion lines that are fit to experimental data. The color map in (c) and (f) were scaled to improve the contrast and visibility of experimentally obtained dispersion lines. The step anomaly at 800 nm in (d) is an experimental artifact due to detector switching in the spectrophotometer.

fore $\vec{a}\cdot\vec{G}^{\parallel}=\vec{a}\cdot(\vec{G}-\vec{G}^{\perp})=\vec{a}\cdot\vec{G}=a_1\vec{A}\cdot\vec{G}+a_2\vec{B}\cdot\vec{G}+a_3\vec{C}\cdot\vec{G}=2\pi(a_1n_1+a_2n_2+a_3n_3)$ and $\vec{b}\cdot\vec{G}^{\parallel}=\vec{b}\cdot(\vec{G}-\vec{G}^{\perp})=\vec{b}\cdot\vec{G}=b_1\vec{A}\cdot\vec{G}+b_2\vec{B}\cdot\vec{G}+b_3\vec{C}\cdot\vec{G}=2\pi(b_1n_1+b_2n_2+b_3n_3)$, where $\vec{G}=\vec{G}^{\perp}+\vec{G}^{\parallel}$.

Since $(a_1n_1+a_2n_2+a_3n_3)$ and $(b_1n_1+b_2n_2+b_3n_3)$ are integers we have proved that $\vec{G}^{\parallel}$ satisfies the Laue equations. This verifies that the projection of $\vec{G}_{200}$ onto the (111) plane, $\vec{G}^{\parallel}_{200}$, is a 2D reciprocal lattice vector within the (111) plane.

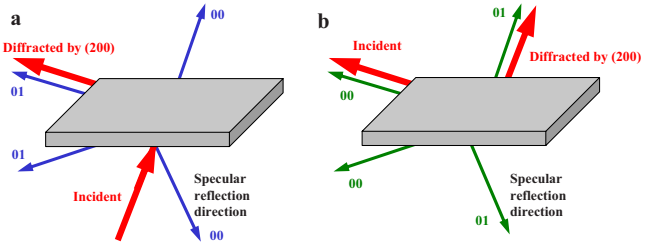

FIG. 2. (Color online) Illustration of a two-step diffraction process resulting in specularly diffracted light from (200) crystal planes about the (111) surface normal. (a) In the first step monochromatic light is incident at 10° about the (111) normal onto the photonic crystal such that it Bragg diffracts from the (200) planes at 99.5° (the incident and 3D diffracted beam are shown by thicker red arrows). The blue arrows show 2D diffraction of the incident light from the hexagonal particle arrays within the (111) planes. The 2D diffraction spectral orders are indicated. Zero-order 2D diffraction occurs in the specular reflection direction. (b) In the second diffraction the 3D Bragg diffracted light by the (200) planes is subsequently 2D diffracted by the particles in the (111) planes. This subsequently 2D diffracted light (green arrows) coincides with the 2D diffraction directions in (a). The 01-order 2D diffraction exits the PhC in the direction of specular reflection about the (111) plane direction.

Figure 3(a) shows two fcc Brillouin-zone surfaces where the (111) surface lies within the rectangular plane shown. The wave vectors $\vec{k}_{in}$ and $\vec{k}_{sc}$ (blue) and $\vec{G}_{200}$ (red) satisfy the 3D Bragg condition $\vec{k}_{sc}=\vec{k}_{in}+\vec{G}_{200}$ forming a triangle. The $\vec{G}_{200}$ reciprocal lattice vector is oriented along the ΓX direction, ending on the 200 reciprocal lattice point. Figure 3(a) shows the projection of these wave vectors ($\vec{k}^{\parallel}_{in}$, $\vec{k}^{\parallel}_{sc}$, and $\vec{G}^{\parallel}_{200}$) onto the (111) plane (blue dashed lines) while Fig. 3(b) concentrates on the 111 Brillouin zone and shows the projected wave vectors onto this surface.

The parallel projections of $\vec{k}_{in}$, $\vec{k}_{sc}$, and $\vec{G}_{200}$ onto the (111) plane forms a triangle:$\vec{k}^{\parallel}_{sc}=\vec{k}^{\parallel}_{in}+\vec{G}^{\parallel}_{200}$ This vector relation indicates the fulfillment of a 2D diffraction condition since $\vec{G}^{\parallel}_{200}$ is a 2D reciprocal lattice vector. This argument proves that the 3D diffraction from the (200) set of planes simultaneously fulfills a 2D diffraction condition within the (111) planes, where the projection, $\vec{G}^{\parallel}_{200}$ is the 2D reciprocal lattice vector.

The (200) diffracted beam, which for a thick photonic crystal has an intensity similar to that of the incident light, propagates within the PhC, and is subsequently diffracted by the 2D periodicity within the (111) planes. The directions of this 2D diffraction are shown by the green arrows in Fig. 2(b) which lie parallel to the Fig. 2(a) 2D diffraction directions shown by the blue arrows.

The 2D diffraction condition is $\vec{k}^{\parallel}_{out}=\vec{k}^{\parallel}_{sc}+\vec{G}^{2D}$, where $\vec{G}^{2D}$ is a reciprocal lattice vector lying within the (111) planes. When $\vec{G}^{2D}=-\vec{G}^{\parallel}_{200}$ the corresponding 2D diffraction beam, $\vec{k}_{out}$, propagates in the specularly reflected direction about the normal to the (111) planes; the parallel projections

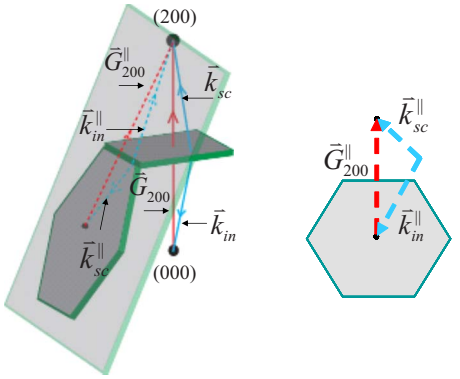

FIG. 3. (Color online) (a) The fcc Brillouin zone is shown with the incident and scattered wave vectors satisfying the diffraction conditions from the (200) planes. $\vec{G}_{200}$ and the incident and scattered wave vectors are projected into the (111) plane. (b) The first Brillouin zone of the (111) planes is shown as are the projections of $\vec{G}_{200}$ into this plane. $\vec{G}^{\parallel}_{200}$ and the projections of the incident and scattered wave vectors together satisfy the 2D diffraction condition. The 2D scattered wave vector lies parallel to the direction of projection of the 3D Bragg diffracted wave vector.

of the incident and specularly reflected beam are equal, $\vec{k}^{\parallel}_{out}=\vec{k}^{\parallel}_{in}$. By combining the diffraction conditions for the first and second scattering events we obtain $\vec{k}^{\parallel}_{out}=\vec{k}^{\parallel}_{sc}-\vec{G}^{\parallel}_{200}=\vec{k}^{\parallel}_{in}+\vec{G}^{\parallel}_{200}-\vec{G}^{\parallel}_{200}=\vec{k}^{\parallel}_{in}$. Therefore, the resultant diffracted beam from these two scattering events propagates in the specularly reflected direction.

Using this result we can understand the origin of the diffraction dispersion lines in Fig. 1. We plot our assigned calculated Bragg dispersion lines on top of the experimentally measured reflection data. We do not observe some of the diffraction dispersion lines that we calculate probably because of their weak intensities.[29]

We observe a well-resolved (020) Bragg dispersion line over the measured angular range which crosses the (111) line. The line crossing occurs at the high-symmetry W point of the Brillouin zone. The calculated and measured dispersion lines overlap completely until the crossing point, whereupon the calculated results begin to deviate significantly from those experimentally observed. The deviation increases as the angles increase past the crossing point, as previously observed by others.[6] This deviation after the crossing point presumably results from our simplistic use of a water and polystyrene volume average refractive index in the Bragg dispersion-line calculations. In addition, we ignore the fact that we are in the dynamical diffraction limit rather than in the kinematic diffraction limit.[30]

The anticrossing behavior of (111) and (200) dispersion lines near their crossing point was studied both experimentally and theoretically by considering simultaneous diffraction by the (111) and (200) planes.[5–7,11–13,31,32] The coupling between these multiple Bragg waves and deviation of the dispersion lines from the simple Bragg's law behavior was explained as a band repulsion of the relevant Bloch eigenstates.[5] The avoided crossing interval between the dispersion lines will increase as the photonic crystal dielectric contrast modulation increases due to an increased coupling

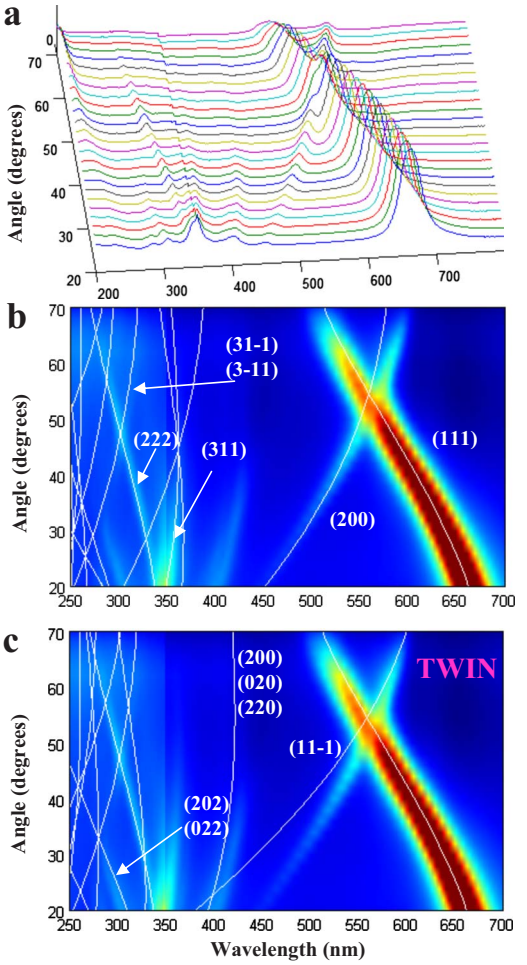

FIG. 4. (Color online) (a) Specularly reflected intensity along the LU (LK) direction for high-concentration CCA. (b) The calculated Bragg dispersion overlaid onto the experimental data contour plot. (c) The Bragg dispersion calculated for twinned crystal configuration.

between the two Bragg diffraction waves.[5] Due to the relatively small dielectric contrast of our CCAs, we observe only a small anticrossing behavior for the (111) and (200) dispersion lines for our high-concentration sample and see little anticrossing behavior for our dilute sample.

We see more dispersion lines then observed previously using either transmission and reflection methods using UV, visible, and near IR light for both close-packed and nonclose-packed PhC, for similar low dielectric constant CCA.[6,8,33] The increased number of dispersion lines we observe may result from better ordering of our highly charged polystyrene CCA PhC.

We also observe good fits between our calculated diffraction dispersion lines and measured dispersion lines for the (13-1), (311) (222), (200), (022), (202), and (113) crystal planes. We are also able to fit the dispersion line observed between 20° and 30° near the intersection of (220) and (11-1) Bragg lines.

Figure 1 shows two additional crossing points at the intersection of the (222) and (13-1), (311) and (113) Bragg lines. These two new dispersion line crossing points are located in the high-energy wavelength region where the com-

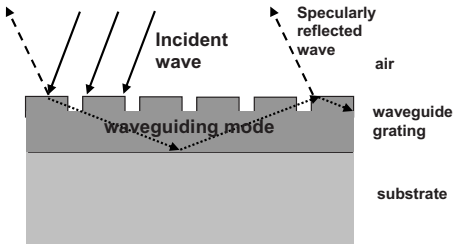

FIG. 5. Wood's anomaly in waveguide grating structure. Light incident at waveguide grating is coupled to the waveguiding mode according to a phase-matching Bragg diffraction. The waveguided mode is diffracted again by the same grating periodicity into the specularly reflected wave.

plete 3D photonic band gap would occur for an inverted fcc CCA with a refractive index contrast >2.8.[34]

Figure 4 shows reflectance spectra obtained for the high-concentration CCA over the angular range $20°-70°$ along the LU (LK) rotation direction. Figure 4(b) shows the calculated Bragg dispersion lines together with the experimental data. Five experimental dispersion lines are in a good agreement with Bragg's law for the diffraction from (111), (200), (311), (222) and simultaneously (31-1) and (3-11) crystal planes. However, two well-resolved dispersion lines remain unaccounted for. The origin of these lines is easily explained as a result from Bragg diffraction of the (200), (020), (220) and (202), (022) crystal planes of a twinned structure. The existence of dispersion lines originating from a twin structure indicates the existence of stacking faults in our CCA sample.

For the LW rotation direction the Bragg dispersion diagram for the fcc crystal and its twin are identical, unlike that for the LU or LK rotation direction. This indicates that for the LW direction it is not possible to distinguish between the dispersion lines of the normal and twin structures.

This multiple diffraction phenomenon is reminiscent the Wood's anomaly known for 1D and 2D dielectric periodic waveguiding grating structures.[19,21] The simplest structure (Fig. 5) which can generate a Wood's anomaly is comprised of a waveguide grating attached to a substrate. Wood's anomalies in these types of structures give rise to sharp peaks in the specularly reflected intensity for particular wavelengths of light at specific angles of incidence. Wood's anomalies are explained by the resonant coupling of the incident light wave to a guided wave which propagates along the waveguide grating. The coupling between the incident and guided waves occurs through the phase-matching Bragg condition $k_G = k_{in} + K$, where k_G and k_{in} are the guided and incident wave-vector projections onto the surface of the grating structure and K is the 1D grating reciprocal lattice vector. Coupling also occurs in the opposite direction, where the guided mode Bragg diffracts through the same phase-matching condition, thus resulting in an intensity peak in the specularly reflecting direction.

Thus, two consecutive diffraction processes occur where the incident and diffracted beams are related through the phase-matching Bragg diffraction. This mechanism is similar to our multiple diffraction model which gives rise to the reflectance peaks in angularly resolved spectra of 3D PhC.

In summary, we show that light diffracted from higher-order Miller-index crystal planes of a fcc photonic crystal in the specularly reflected direction about the normal to the (111) planes results from a multiple diffraction phenomenon. This phenomenon is a result of a two-step diffraction process whereby light is Bragg diffracted by a higher-order Miller-index crystal plane and also 2D diffracted by 2D periodicities within the (111) planes. We suggest that this phenomenon is an analog of the Wood's anomaly in diffracting grating structures.

We greatly acknowledge funding from NSF Grant No. CHE-0848265.

*Author to whom correspondence should be addressed. FAX: 412-624-0588; asher@pitt.edu

[1] J. D. Joannopoulos *et al.*, Nature (London) **387**, 830 (1997).
[2] E. Yablonovitch, Phys. Rev. Lett. **58**, 2059 (1987).
[3] S. John, Phys. Rev. Lett. **58**, 2486 (1987).
[4] W. L. Vos and H. M. van Driel, Phys. Lett. A **272**, 101 (2000).
[5] H. M. van Driel and W. L. Vos, Phys. Rev. B **62**, 9872 (2000).
[6] S. Schutzmann *et al.*, Opt. Express **16**, 897 (2008).
[7] S. G. Romanov *et al.*, Phys. Rev. E **63**, 056603 (2001).
[8] R. D. Pradhan *et al.*, Phys. Rev. B **55**, 9503 (1997).
[9] E. Pavarini *et al.*, Phys. Rev. B **72**, 045102 (2005).
[10] H. Miguez *et al.*, Appl. Phys. Lett. **84**, 1239 (2004).
[11] M. Ishii *et al.*, Colloids Surf., B **56**, 224 (2007).
[12] J. F. Galisteo-Lopez *et al.*, Phys. Rev. B **68**, 115109 (2003).
[13] G. M. Gajiev *et al.*, Phys. Rev. B **72**, 205115 (2005).
[14] A. V. Baryshev *et al.*, Phys. Rev. B **76**, 014305 (2007).
[15] S. G. Romanov *et al.*, Appl. Phys. Lett. **92**, 191106 (2008).
[16] L. C. Andreani *et al.*, Phys. Rev. B **78**, 205304 (2008).
[17] J. F. Galisteo-Lopez and C. Lopez, Phys. Rev. B **70**, 035108 (2004).
[18] R. W. Wood, Philos. Mag. **4**, 396 (1902).
[19] A. Hessel and A. A. Oliner, Appl. Opt. **4**, 1275 (1965).
[20] S. S. Wang *et al.*, J. Opt. Soc. Am. A **7**, 1470 (1990).
[21] D. Rosenblatt *et al.*, IEEE J. Quantum Electron. **33**, 2038 (1997).
[22] S. Fan and J. D. Joannopoulos, Phys. Rev. B **65**, 235112 (2002).
[23] C. E. Reese *et al.*, J. Colloid Interface Sci. **232**, 76 (2000).
[24] P. L. Flaugh *et al.*, Appl. Spectrosc. **38**, 847 (1984).
[25] R. J. Carlson and S. A. Asher, Appl. Spectrosc. **38**, 297 (1984).
[26] Stacking faults in fcc CCA would result in loss of the ability to distinguish the twinned CCA LU and LK directions (Ref. 16). Thus, we will refer to this direction as a LU (LK) direction. In our experiment we achieved CCA orientation along the LU (LK) direction by rotating the CCA 30° along the LΓ axis.
[27] W. Loose and B. J. Ackerson, J. Chem. Phys. **101**, 7211 (1994).
[28] A. V. Baryshev *et al.*, Phys. Rev. B **73**, 205118 (2006).
[29] F. Lopez-Tejeira *et al.*, Phys. Rev. B **65**, 195110 (2002).
[30] B. T. Schwartz and R. Piestun, J. Opt. Soc. Am. B **22**, 2018 (2005).
[31] J. F. Galisteo Lopez and W. L. Vos, Phys. Rev. E **66**, 036616 (2002).
[32] A. V. Baryshev *et al.*, Phys. Rev. B **73**, 033103 (2006).
[33] I. I. Tarhan and G. H. Watson, Phys. Rev. Lett. **76**, 315 (1996).
[34] K. Busch and S. John, Phys. Rev. E **58**, 3896 (1998).